TAO, Vol. 10, No. 4, 873-883, December 1999

A Comparison of OCI and SeaWiFS Satellite Imagery in the Waters Adjacent to Taiwan

Hsien-Wen Li[1], Chung-Ru Ho[1], Nan-Jung Kuo[1], Chun-Te Chen[2], and Wei-Peng Tsai[1]

(Manuscript received 29 September 1999, in final form 19 November 1999)

ABSTRACT

With the successful launch of the first scientific satellite of the Republic of China (ROCSAT-1) on 27 January 1999, Taiwan enters the era as a satellite data providing country. There are three scientific payloads on the satellite. One of them is the Ocean Color Imager (OCI). OCI is a push-broom reflective imager for monitoring ocean colors. OCI has taken images since March 1999. Because there is no on-board calibrator on OCI, a comparison with Sea-viewing Wide Field-of-view Sensor (SeaWiFS) data was performed in order to validate OCI data. Simultaneously in-situ observations of optical properties and chlorophyll *a* concentration were also collected in waters adjacent to Taiwan for vicarious calibration. We applied SeaWiFS atmospheric correction and bio-optical algorithms on OCI data to derive normalized water-leaving radiance and chlorophyll *a* concentration. Results show that the chlorophyll *a* concentration derived from OCI is generally larger than that derived from SeaWiFS. The correlation coefficient is about 0.60 with a root-mean-squared (RMS) of difference of chlorophyll *a* concentration of 0.10 mg/m^3.

(Key words: OCI, SeaWiFS, Validation, Ocean color, SIMBIOS)

1. INTRODUCTION

With the successful launch of the first scientific experimental satellite of the Republic of China (ROCSA-1) on 27 January 1999, Taiwan enters the era of satellite data providing country. The satellite is designed to carry out three scientific experiments: ocean color imaging, ionospheric plasma and electrodynamics, and Ka-band communication. The payload instrument for ocean color imaging on ROCSAT-1 is called the Ocean Color Imager (OCI). OCI is a nadir-viewing push-broom imager, designed to map reflected spectral radiance from ocean surfaces in six visible and near infrared bands. From the remote sensing point of view, ocean color is the relative amounts of water-leaving radiance in various portions of the visible spec-

[1]Department of Oceanography, National Taiwan Ocean University, Keelung, Taiwan, ROC
[2]Department of Fishery Science, National Taiwan Ocean University, Keelung, Taiwan, ROC

trum. Measurements of water-leaving radiance allow concentrations of chlorophyll *a* to be derived.

After the successful launch of SeaWiFS in August 1997 has provided a very good opportunity to perform in-flight calibration and validation for both sensors by the intercomparison method, especially for OCI because it has no on-board calibrator. For sensors without on-board calibration capabilities, indirect methods are the only ways available to monitor calibration coefficients while the instruments operate in orbit. The intercomparison work between OCI and SeaWiFS is also a part of the Sensor Intercomparison and Merger for Biological and Interdisciplinary Oceanic Studies (SIMBIOS) project, organized by the National Aeronautics and Space Administration (NASA).

For calibration and validation purposes, images are scheduled to be taken simultaneously when OCI tracks overlap with SeaWiFS, or the calibration buoy location or the location of the experimental cruises. To achieve radiance from the ocean, space-borne ocean color sensors require several levels of radiometric calibration. It includes gain-offset correction, which converts digital counts into at-sensor radiance (Schowengerdt, 1997) and atmospheric correction, which transforms at-sensor radiance into water-leaving radiance. In this study, we applied the SeaWiFS atmospheric correction and bio-optical algorithms on OCI data, and then compared the results with quasi-simultaneous SeaWiFS data. The results help us to better understand the quality of OCI and its difference from SeaWiFS.

2. DESCRIPTION OF OCI

OCI is a push-broom reflective and nadir-viewing imager. It is designed to map reflected spectral radiance from ocean surfaces in seven visible and near-infrared (NIR) bands. The seven spectral bands actually cover six independent wavebands. The central wavelengths of the seven bands are 443 nm, 490 nm, 510 nm, 555 nm, 670 nm, 865 nm and 555 nm, and are denoted as Band 1, 2, 3, 4, 5, 6 and 7, respectively. The Band 7 is a redundancy of Band 4. It is used for inter-track radiance and calibration purposes. Since the constraints on total mass and envelope of ROCSAT-1, OCI has been designed and implemented with seven spectral bands to share four telescopes. Bands 1 and 3 get radiance from the same telescope. Bands 2 and 4 and Bands 5 and 6 are another two pairs. Band 7 has a stand-alone telescope. A comparison of characteristics between SeaWiFS and OCI is listed in Table 1.

OCI focal planes are of Thomson's 1728-element linear charge-coupled device (CCD) sensors. This kind of sensor is designed to have a distinctive anti-blooming feature. With a nominal telescope focal length of 19.5 mm and a photosite pitch of 13 μm square, an instantaneous field of view (IFOV) covers 2 CCD pixels. Therefore, an 800 by 800 square meter footprint on the ground is formed by the push-broom action. The swath of OCI is about 700 km. A detailed description of OCI characteristics can be found in Lee et al. (1999).

3. VALIDATION

It is believed that the OCI calibration at each wavelength will change in some unpredict-

Table 1. A comparison of characteristics between SeaWiFS and OCI.

	SeaWiFS	OCI
Inclination	98.25°	35°
Altitude (km)	705	600
Period (min)	98.9	96.6
Orbital repeat time (days)	16	52
Spectral bands (nm)	B1 402-422 B2 480-500 B3 480-500 B4 500-520 B5 545-565 B6 660-680 B7 745-785 B8 845-885	B1 433-453 B2 433-453 B3 500-520 B4 545-565 B5 660-680 B6 845-885 B7 545-565
Nadir pixel (m^2)	1130 x 1130	800 x 800
Swath width (km)	2801	702
Color sensing	scanner	push broom
Crossing equator time (local time)	12:00	anytime
Tilt	-20°, 0°, 20°	No
Launch date (year/month)	1997/8	1999/1

able manners as a function of time. Experience with previous sensors, such as the Coastal Zone Color Scanner (CZCS), has shown that it is very difficult to determine a sensorís calibration once it has been launched (Mueller and Austin, 1992). To validate OCI data, in situ measurements of optical properties were carried out with a Tethered Spectral Radiometer Buoy (TSRB-II) and a SeaWiFS Profiling Multi-channel Radiometer (SPMR) made by Satlantic Company. TSRB-II is an optical buoy, which can measure the in-water upwelling radiance just beneath the sea surface $L_u(0^-,\lambda)$ and the incident spectral irradiance above the sea surface $E_s(\lambda)$. SPMR is a profiling radiometer that can measure the in-water upwelling radiance $L_u(z,\lambda)$ and downwelling spectral irradiance $E_d(z,\lambda)$ with depth z. Originally these instruments were developed for SeaWiFS data validation. Since OCI has similar band characteristics to SeaWiFS, we can also used these instruments for OCI data validation. All of these in situ measurement instruments have the same wavelength in visible bands as those of SeaWiFS

and OCI.

To obtain $L_u(z,\lambda)$ that is measured by the OCI, it is necessary to propagate $L_u(0^-,\lambda)$ upward through the sea surface as

$$L_w(\lambda) = L_u(0^-,\lambda)\frac{1-\rho(\lambda,\theta)}{n_w^2(\lambda)}, \tag{1}$$

where $\rho(\lambda,\theta)$ and $n_w(\lambda)$ are the Fresnel reflectance at the solar zenith angle θ and the refractive index for seawater, respectively. In order to remove the influence of view angle, sun angle and the solar irradiance, the water-leaving radiance is generally transferred to the normalized water-leaving radiance L_{wn} as

$$L_{wn}(\lambda) = L_w(\lambda)\frac{\overline{F}_0(\lambda)}{E_s(\lambda)}, \tag{2}$$

where $\overline{F}_0(\lambda)$ denotes the mean extraterrestrial solar irradiance (Neckel and Labs, 1984). For calculating the remote sensing reflectance just above the sea surface $R_{rs}(\lambda)$, the following equation was used (O'Reilly et al., 1998)

$$R_{rs}(\lambda) = \frac{0,54L_u(0^-,\lambda)}{E_s(\lambda)}, \tag{3}$$

The bio-optical algorithm for chlorophyll *a* concentration calculation from $R_{rs}(\lambda)$ is given by

$$C = 10^{(0.2974-2.2429R+0.8358R^2-0.0077R^3)} - 0.0929, \tag{4}$$

where C is chlorophyll *a* concentration, and R is defined as

$$R = \log(R_{rs}(490)/R_{rs}(555)). \tag{5}$$

3.2 SeaWiFS Algorithms

The total upward radiance at the top of the ocean-atmosphere system, measured at a wavelength l, can be written as

$$L_t(\lambda) = L_r(\lambda) + L_a(\lambda) + L_{ra}(\lambda) + t(\lambda)L_{wc}(\lambda) + t(\lambda)L_w(\lambda), \tag{6}$$

where $L_r(\lambda)$ is the radiance from multiple scattering by air molecules, $L_a(\lambda)$ is the radiance from multiple scattering by aerosols, $L_{ra}(\lambda)$ is multiple interaction between molecules and aerosols, and $L_{wc}(\lambda)$ is the radiance at the sea surface that arises from sunlight and skylight reflecting from whitecaps on the surface (Gordon and Wang, 1994). The $t(\lambda)$ is the diffuse transmittance which accounts the effects of propagating water-leaving radiance and whitecap reflectance from the sea surface to the top of the atmosphere. Since SeaWiFS has a tilt func-

tion to avoid the effect of sun glitter, in Eq. (6) the surface sun glitter term has been ignored. For OCI, the term of sun glitter has to be taken into account, because it has no tilt function.

The goal of the atmospheric correction is to retrieve the $L_w(\lambda)$ accurately from the spectral measurements of radiance at the satellite. To relate the derived $L_w(\lambda)$ to the ocean inherent optical properties, the atmospheric effects on the $L_w(\lambda)$ must removed. The $L_w(\lambda)$ can be defined from Gordon and Clark (1981),

$$L_{wn}(\lambda) = L_w(\lambda)/\cos\theta\, t(\lambda,\theta), \tag{7}$$

where $t(\lambda,\theta)$ is the atmospheric diffuse transmittance in the solar direction with the solar zenith angle. To determine the term of $t(\lambda,\theta)$, the atmospheric correction algorithm for SeaWiFS was developed by the SeaWiFS team (Wang and Gordon, 1994). After doing the atmospheric correction on SeaWiFS data, the $L_{wn}(\lambda)$ measured from SeaWiFS was then derived.

3.3 Match-up Data Set

There were six optical data and water samples taken in the waters adjacent to Taiwan from October 1998 to June 1999. These data were measured when SeaWiFS flights over the filed measurement areas within three hours. There are three data sets whose time lag is less than one hour. The information related to in-situ measurements and SeaWiFS images are listed in Table 2. Measurements on each cruise include profiles of $E_d(z,\lambda)$ and $L_u(z,\lambda)$, and $E_s(\lambda)$ at SeaWiFS wavelengths, as well as fluorometric chlorophyll *a* concentration from water samples. Radiometric profiles are analyzed to obtain $L_u(0^-,\lambda)$, and then $L_{wn}(\lambda)$ is derived by Eqs. (1) and (2). Chlorophyll *a* concentration is then dervied from Eqs. (3), (4), and (5).

Figure 1 shows a comparison of L_{wn} at 412 nm, 443 nm, 490 nm, 510 nm and 555 nm, as well as chlorophyll *a* concentration derived from SeaWiFS data and in-situ measurements. From Fig. 1 we can see that correlation coefficients of SeaWiFS derived products and in-situ

Table 2. Information of match-up data sets.

In-situ Measurements				SeaWiFS File Names
Date	Time (UTC)	Latitude (°)	Longitude (°)	
10/01/98	04:39	21.80	121.90	S1998274042206.L1A_HNTO
11/03/98	05:43	22.37	120.16	S1998307041427.L1A_HNTO
11/05/98	03:08	22.10	120.53	S1998309040521.L1A_HNTO
05/11/99	07:27	25.07	120.87	S1999131044101.L1A_HNTO
05/14/99	02:45	26.15	121.46	S1999134033615.L1A_HNTO
06/01/99	04:08	24.53	119.83	S1999152034621.L1A_HNTO

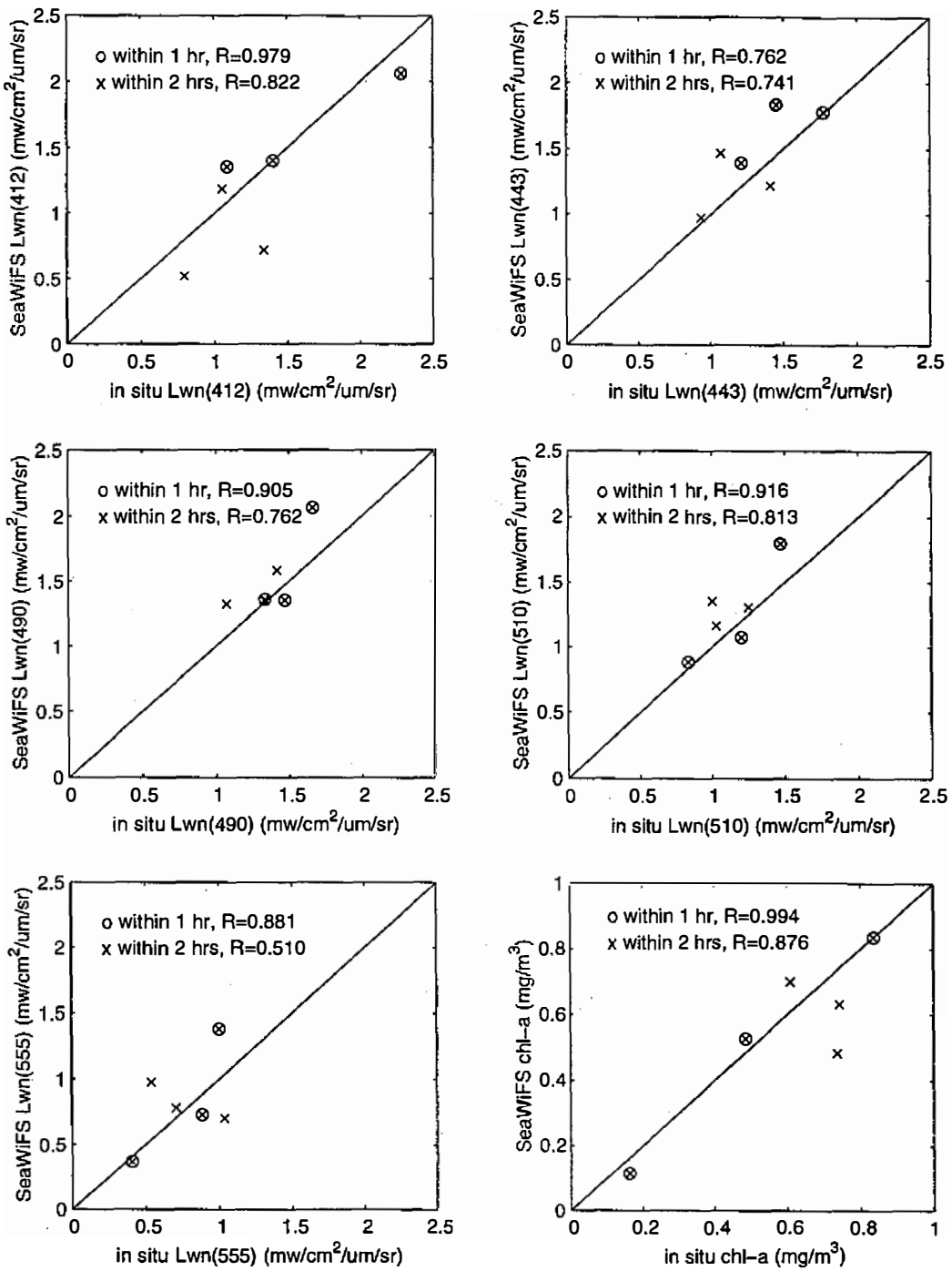

Fig. 1. A comparison of L_{wn} and chlorophyll *a* concentration derived from SeaWiFS data and in-situ measurements.

measurements are high, especially for chlorophyll *a* concentration. The correlation coefficient of chlorophyll *a* concentration is as high as 0.994, when the difference in measuring time between SeaWiFS and in-situ is within one hour. Therefore we will compare the chlorophyll *a* concentration derived from OCI with that derived from SeaWiFS.

4. COMPARISON WITH SeaWiFS DATA

A way to validate OCI data products is by intercomparison with data from other spaceborne ocean color sensors. The difficulties of this method, however, are spectral matching, ground spatial resolution, and sun-sensor geometry (Che, 1991). Unlike SeaWiFS on SeaStar, it takes images near local noon. ROCSAT-1 is not a sun-synchronous satellite, it is on a 35° inclination. Hence OCI can take images anytime in a day. Theoretically, we should have simultaneous OCI and SeaWiFS images every day. However, in order to avoid the effect of sun glint, SeaWiFS has a 20° forward or backward tilting, but OCI does not have this function. To avoid sun glint effect on OCI images, OCI takes image in the early morning or in the late afternoon. Therefore, it is not easy to obtain simultaneous images of SeaWiFS and OCI, both of which have the same view angle and sun angle at the nadir point. We can not compare the total radiance received by the ocean color sensors. For intercomparison, we adopted quasi-simultaneous images and assumed that parameters in the ocean do not change much within a short time. Thus, if we apply the SeaWiFS atmospheric correction algorithm and the bio-optical algorithm on OCI, we can intercompare the chlorophyll *a* concentration, which is not affected by the sensor view angle and sun angle.

As we know, different ocean color sensors usually have different band spectral characterizations. It is difficult to apply one atmospheric correction algorithm to other sensors. According to the evaluation of accuracy of the SeaWiFS atmospheric correction algorithm for various ocean color sensors (Wang, 1999), the SeaWiFS atmospheric correction can be applied to other color sensors for solar zenith angles less than 60°. Therefore, we can perform the SeaWiFS atmospheric correction algorithm on OCI data and have the same accuracy as SeaWiFS, if we have pixels on the OCI images in which sun zenith angles are less than 60°.

Figure 2a is an image of chlorophyll *a* concentration derived from OCI data taken at 00:24 (UTC) of April 16, 1999. The area of this image is near Taiwan. Figure 2b is a SeaWiFS chlorophyll *a* concentration image received at 04:15 (UTC) on the same day as Fig. 2a by the receiving station at National Taiwan Ocean University (NTOU). The area is also around Taiwan. We can see that some oceanic features, such as meanders on the Luzon Strait, can be easily found on the enhanced images (Figs. 3a and 3b). Another example for comparison between OCI and SeaWiFS is shown on Fig. 4. Figure 4a is an image of chlorophyll *a* concentration derived from OCI data taken at 02:11 (UTC) of May 17, 1999. We can see that there is an eddy-like feature (marked A) with higher chlorophyll *a* concentration in the northern South China Sea. This feature (marked A) is also seen on the SeaWiFS image (Fig. 4b) taken at 04:11 (UTC) of May 17, 1999. From the above examples, we may conclude that OCI data qualitatively stands comparison with SeaWiFS data, and can be used for some oceanic dynamical studies. Next, we will compare OCI and SeaWiFS quantitatively.

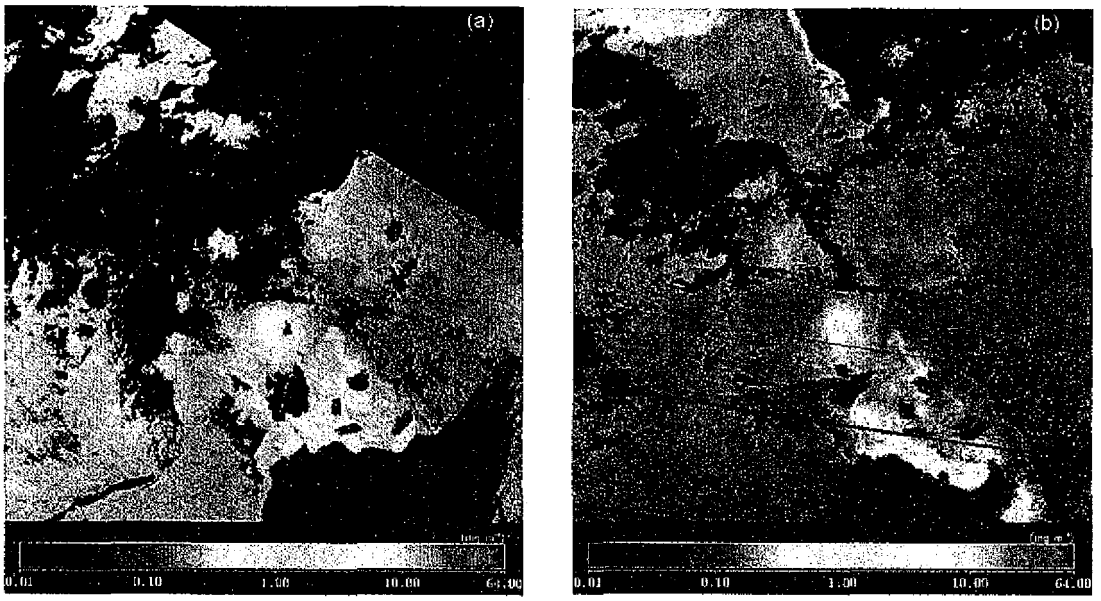

Fig. 2. (a) An image of chlorophyll *a* concentration derived from OCI data taken at 00:24 (UTC) of April 16, 1999. (b) Same as (a), but derived from SeaWiFS data taken at 04:15 (UTC) of April 16, 1999.

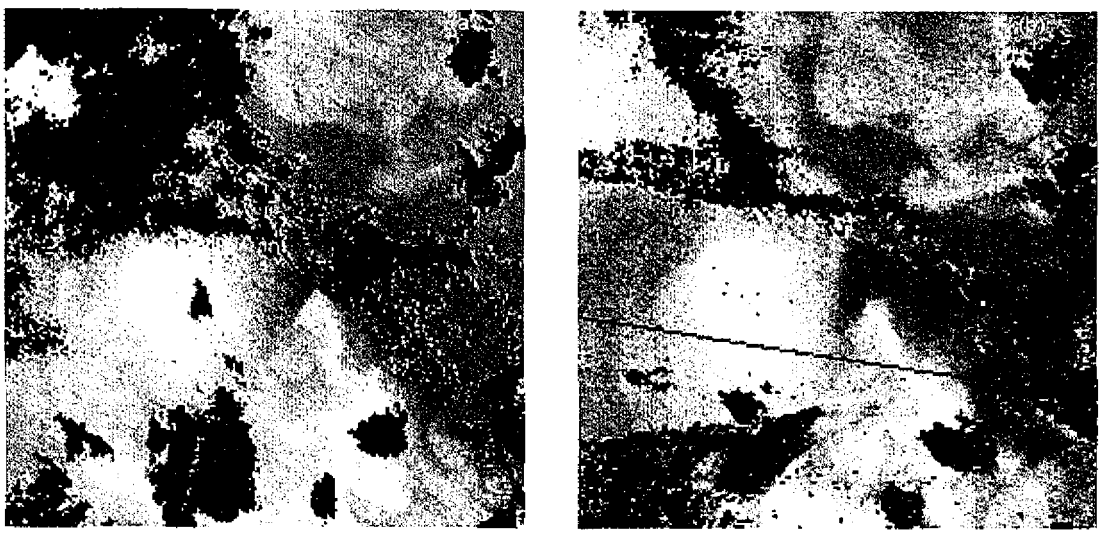

Fig. 3. (a) Enhanced image of Fig. 2a. (b) Same as (a), but for Fig. 2b.

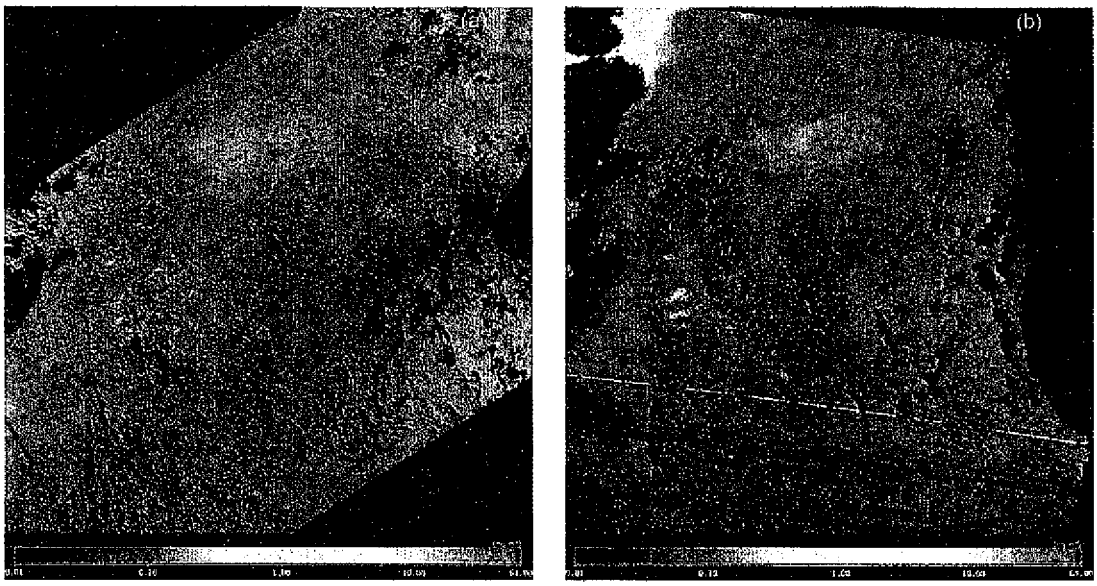

Fig. 4. (a) Chlorophyll *a* concentration image taken by OCI at 02:11 (UTC) of May 17, 1999. (b) Same as (a), but taken by SeaWiFS at 04:11 (UTC) of May 17, 1999.

After performing geometrical correction and the Mercator projection, we produced the same spatial resolution for SeaWiFS and OCI images. We performed the SeaWiFS atmospheric correction algorithm on OCI in order to do the intercomparison. Only pixels in which sun zenith angles were less than 60° were used for comparison. We then applied the SeaWiFS bio-optical algorithm to OCI data to derive the chlorophyll *a* concentration. There were four pairs of chlorophyll *a* concentration from OCI and SeaWiFS for intercomparison. These imageries were taken in the waters adjacent to Taiwan. The range of chlorophyll *a* concentration is from 0.01 mg/m^3 to 3.0 mg/m^3. The differences of measuring time for OCI and SeaWiFS are within four hours. From Fig. 5 we can see that the chlorophyll *a* concentration derived from OCI is generally larger than that derived from SeaWiFS. For Fig. 5a, the difference of measuring time between OCI and SeaWiFS is about two and half an hours. The average ratio of OCI chlorophyll *a* concentration to SeaWiFS is about 2.3. For Fig. 5b, the time difference is about four hours. The average ratio of OCI and SeaWiFS is about 2.7. For Fig. 5c, the difference of time is about two hours. The average ratio is reduced to 1.3. For Fig. 5d, the time difference is about three hours. The average ratio is about 1.6. From the comparison, we find that, if the imaging time for both sensors is close, the result is better. We also computed the correlation coefficient of chlorophyll *a* concentration between OCI and SeaWiFS for available data, for which the difference of measuring time is within four hours. It is about 0.60 with a root-mean-squared (RMS) of difference of chlorophyll *a* concentration of 0.10 mg/m^3.

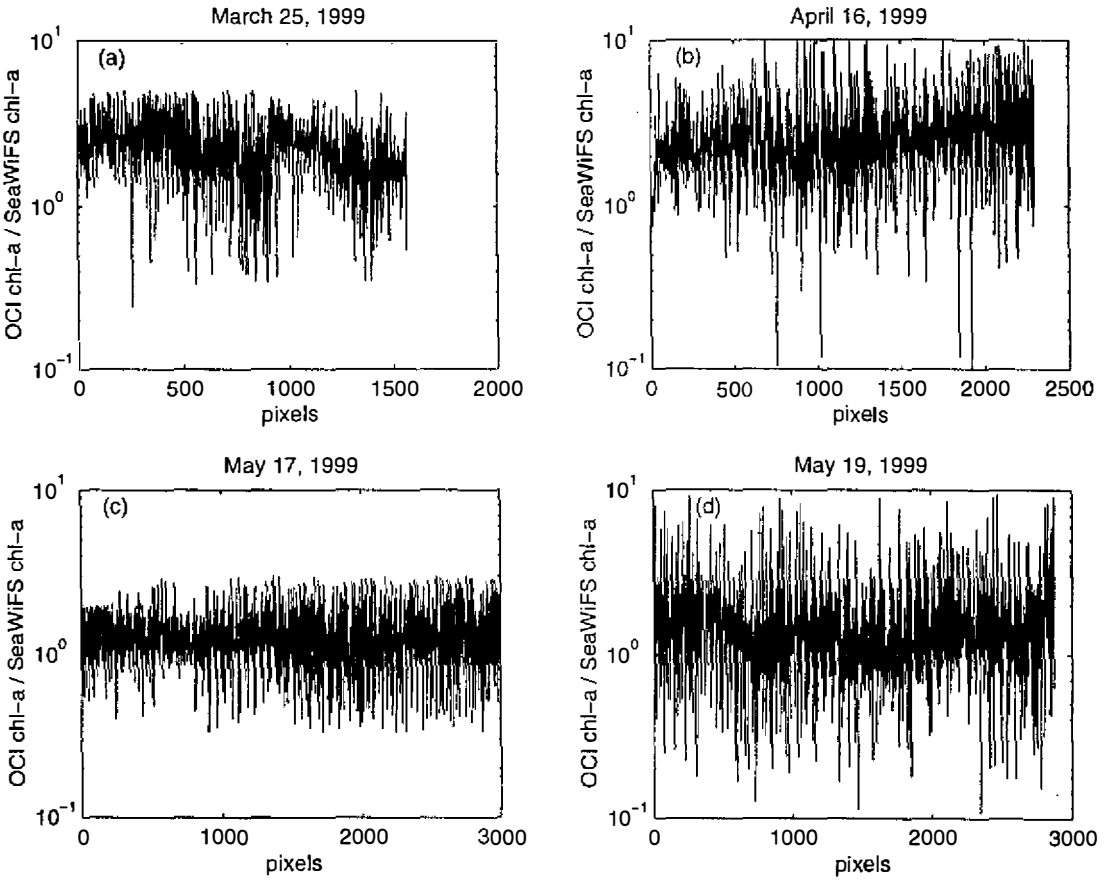

Fig. 5. A comparison of chlorophyll *a* concentration derived from SeaWiFS and OCI data. (a) March 25, 1999, (b) April 16, 1999, (c) May 17, 1999, and (d) May 19, 1999.

5. DISCUSSION AND CONCLUSIONS

OCI is the first space-borne ocean color sensor in Taiwan. From the OCI images obtained, we found that the quality of OCI images is acceptable. Oceanic features on SeaWiFS images can also be found on OCI images. OCI data qualitatively bear comparison with SeaWiFS data. From the quantitative comparison we found that the chlorophyll *a* concentration derived from OCI using SeaWiFS atmospheric correction and bio-optical algorithms is larger than that derived from SeaWiFS data. Generally speaking, the correlation coefficient of chlorophyll *a* concentration between OCI and SeaWiFS is 0.60. We believe that the sensor calibration and the difference of imaging time caused the difference between OCI and SeaWiFS. To calibrate and validate OCI data, in-situ measurements of optical properties and chlorophyll *a* concentration are still necessary. The comparison of OCI with SeaWiFS is also a good way for OCI data validation. The engineers of NSPO and the OCI science team are still working on the sensor

calibration. A better quality of OCI data can be expected in the near future. OCI data can be requested through the web site of the OCI Science Data Distribution Center (SDDC) at http://www.oci.ntou.edu.tw/.

Acknowledgments Many thanks go to captains and crew of R/V Ocean Researcher II and R/V Ocean Researcher III for shipboard assistance. We also thank Mr. Hong-Ann Chen, Miss Wen-Chen Su, and Miss Hua-Huei Huang for processing OCI and SeaWiFS data, as well as in-situ data. We appreciate the assistance of the GSFC/DAAC of NASA for providing the SeaWiFS data. This work is supported by the National Space Program Office (NSPO) under grants NSC83-NSPO-A-RDD-019-002, NSC84-NSPO-(A)-OCI-001-02, NSC85-NSPO-(A)-OCI-019-02, NSC86-NSPO-(A)-OCI-019-01, NSC86-NSPO-(A)-OCI-019-02, NSC87-NSPO-(A)-OCI-019-01, NSC87-NSPO-(A)-OCI-019-02, NSC88-NSPO-(A)-OCI-019-01, and NSC88-NSPO-(A)-OCI-019-02.

REFERENCES

Che, N. B., B. G. Grant, D. E. Flittner, P. N. Slater, S. F. Biggar, R. D. Jackson, and M. S. Moran, 1991: Results of calibration of the NOAA-11 AVHRR made by reference to calibrated SPOT imagery at White Sands, N. M., *SPIE: Calibration of Passive Remote Observing Optical and Microwave Instrumentation*, **1493**, 182-194.

Gordon, H. R., and D. K. Clark, 1981: Clear water radiances for atmospheric correction of coastal zone color scanner imagery. *Appl. Opt.*, **20**, 4175-4180.

Gorden, H. R., and M. Wang, 1994: Influence of oceanic whitecaps on atmospheric correction of ocean-color sensor. *Appl. Opt.*, **33**, 7754-7763.

Lee, L. S., K. Lo, and Y. J. Chiang, 1999: Ocean color imager: instrument description and its performance. *TAO Suppl.*, 43-61.

Mueller, J. L., and R. W. Austin, 1992: Ocean optics protocols for SeaWiFS validation. NASA Tech. Memo., 104566, Vol. 5. In: S. B. Hooker and E. R. Firestone (Eds.), NASA Goddard Space Flight Center, Greenbelt, Maryland, 43 pp.

Neckel, H., and D. Labs, 1984: The solar radiation between 3,300 and 12,500 A. *Solar Phys.*, **90**, 205-258.

O'Reilly, J. E., S. Maritorena, B. G. Mitchell, D. A. Siegel, K. L. Carder, S. A. Garver, M. Kahru, and C. McClain, 1998: Ocean color chlorophyll algorithms for SeaWiFS. *J. Geophys. Res.*, **103**, 24937-24953.

Schowengerdt, R. A., 1997: Remote sensing: models and methods for image processing, 2nd ed., Academic Press, New York, 522 pp.

Wang, M., 1999: A sensitivity study of the SeaWiFS atmospheric correction algorithm: effects of spectral band variations. *Remote Sens. Environ.*, **67**, 348-359.

Wang, M., and H. R. Gordon, 1994: A simple, moderately accurate, atmospheric correction algorithm for SeaWiFS. *Remote Sens. Environ.*, **50**, 231-239.